Hydro-geochemical characterization and water quality appraisal of groundwater in areas adjoining primordial landfills in the Maastrichtian Lafia Formation, Middle Benue Trough

S. E. Obrike[1,2] · L. D. Aleku[2,3] · G. K. Anudu[1,2]

Received: 10 May 2022 / Accepted: 11 July 2022

Abstract
This study assessed the groundwater quality in areas adjoining primordial landfills in Lafia town and its suitability for drinking purposes. Physico-chemical properties of twenty groundwater samples collected from boreholes, unlined and lined hand-dug wells at twenty different locations around three dumpsites were analysed for the appraisal of the water quality. Results of measured physical parameters show pH values in the range of 5.13–7.30, electrical conductivity (EC) values as between 89 and 7754 µS/cm and total dissolved solids (TDS) values that ranges from 59.63 to 5195 mg/L. The major cation and anions have mean concentrations in the order $Ca^{2+} > Na^{+} > K^{+} > Mg^{2+}$ and $SO_4^{2-} > HCO_3^{-} > Cl^{-} > CO_3^{-}$. The Piper plot reveals three dominant water types (Ca–Cl–SO_4, Ca–Na–HCO_3^{-}, and Na–Cl–SO_4). Heavy metal pollution assessment reveals relatively higher modified heavy metal index (m-HMI) values for wells of close proximity to the landfills. The water quality index (WQI) classification reveals 35% of the groundwater sampled locations have water categorized as unsuitable for drinking purposes, 30% of the groundwater samples categorized as very poor and 25% of the groundwater samples classified as poor. While groundwater categorized as good to excellent constituted only 10% of the total groundwater samples analysed.

Keywords Hydro-geochemical · Groundwater quality · Landfills · Cluster analysis

Introduction

Periodic groundwater quality evaluation is vital for assessing groundwater suitability for industrial and domestic purposes. This is particularly important when the water is suspected to have been contaminated due to natural processes or anthropogenic activities. Indiscriminate solid waste disposals and wastewater discharges are two notable anthropogenic activities in developing countries of sub-Saharan Africa that may pose considerable threats to the area's groundwater resource. Sites designated as landfills that were initially situated in the outskirts of some ancient cities have gradually found their way into the city's mainstream urban centres as a result of poor urban planning and rapid population growth. These traditional landfills which were essentially open dumps of either area, trench, ramp or slope landfill methods, are, however, not sanitary in nature. Consequently, the effects of emanating leachates from landfills on groundwater in these areas can be extensive. Lafia town prior to becoming the capital of Nasarawa State, Nigeria, was largely a linear settlement centred around its main market, the emir's palace and along the Lafia—Awe and Lafia—Makurdi roads. However, the city's new status as a state administrative capital has resulted in rapid growth in population and infrastructural development. Supplies of treated pipe-borne water from the Doma dam is generally seen to be inadequate for the growing populace and water obtained from precipitation, in streams and rivers are periodically scarce during the intense dry seasons (Essien et al., 2011; Offodile, 1976, 1989). Consequently, an attendant increased reliance on groundwater sources within the city is common. Natural groundwater chemistry is made-up of dissolved cations, anions and trace elements that constitute about 90% of its total dissolved solids (TDS) contents (Subba Rao, 2006). Usually, heavy metal

✉ S. E. Obrike
steveobrike@nsuk.edu.ng; zobrike@gmail.com

[1] Institute of Geosciences and Earth Resources, Nasarawa State University, Keffi, Nigeria

[2] Department of Geology and Mining, Nasarawa State University, Keffi, Nigeria

[3] Geochemistry and Hydrogeology, University of Bremen, Bremen, Germany

Published online: 27 July 2022

contamination is of great concern due to its toxicity, perseverance and bioaccumulation character. Concentration of trace elements in groundwater owing to anthropogenic activities, is commonly raised to levels that could be harmful to human health on consumption. For this purpose, guidelines and standards were established by water quality monitoring organizations such as Nigerian Standard for Drinking Water Quality (NSDWQ), United States Environmental Protection Agency (USEPA) and World Health Organization (WHO). These guidelines/standards aim to prescribe the minimum or reasonable requirements for safe practices in the interest of consumers' health. The guidelines/standards are usually in the form of numerical values for water constituents or water quality indicators (WHO, 2017). In addition to the common hydro-geochemical approach to groundwater evaluation, a number of new techniques have been integrated by various authors to achieve more robust water quality assessments. Examples of which are multivariate statistics (Kumar et al., 2014, 2015), water evaluation indices (Bodrud-Doza et al., 2016; Dash et al., 2019), heavy metal indices and health risk assessment (Barzegar et al., 2018; Egbueri et al., 2020; Igwe & Omeka, 2021). All of the foregoing have provided a better understanding of the processes that influence groundwater quality which in turn is central in the planning, monitoring and management of groundwater resource. Hence, this study assessed the groundwater quality in areas adjoining three landfills in the study area based on the modified heavy metal pollution and the water quality indices with a view to ascertaining its suitability for domestic and drinking purposes.

Materials and methods

Regional geological setting

The Benue Trough is an elongate linear intra-cratonic rift basin formed in the Late Jurassic to Early Cretaceous (Anudu & Obrike, 2021; Burke & Dewey, 1974; Burke & Whiteman, 1973; Fairhead & Binks, 1991; Guiraud & Maurin, 1992, 1993; Guiraud et al., 2005; Nwajide, 2013; Olade, 1975; Wright, 1976, 1981). This mega-shear structure with a NNE-SSW trend extends for about 800 km length-wise and a width of about 150 km. The Trough is comprised of several NE–SW trending pull-apart sub-basins arbitrarily partitioned into lower, middle and upper segments and is filled with Cretaceous to Tertiary sediments (Anudu et al., 2020; Benkhelil et al., 1988, 1989; Nwajide, 2013; Obaje, 2009; Zaborski, 1998). The entire Trough (though at varying degrees) had experienced two major episodes of compressional folding (Cenomanian and Santonian) culminating in the folding, faulting and upliftment of the pre-Santonian successions (Nwajide, 2013; Zaborski, 1998). The middle segment of the Trough is comprised of seven pull-apart sub-basins (depocentres) which serves as reservoir for upwards of 2500–3100 m of Cretaceous (Albian—Maastrichtian) sediments of both marine and continental origin (Anudu, et al., 2020; Benkhelil et al., 1988, 1989).

Stratigraphically, the Albian Asu River group sediments comprised of the Arufu limestone, the Uomba Formation and the Gboko limestone are the oldest and form basal sediments in the middle segment of the Trough. These basal sediments directly overlie the basement unconformably (Offodile & Reyment, 1977). The Asu River group is overlain by the transitional marine to fluviatile, Late Albian to Early Cenomanian Awe Formation made-up of flaggy fine to medium grained sandstones with interbeds of salt-rich carbonaceous clays and shale (Nwajide, 2013; Obaje, 2009; Offodile, 1989; Zaborski, 1998). The fluvio-deltaic sediments of the Keana Formation were deposited during the Late Cenomanian to Early Turonian. The sediments of the Keana Formation overlie the Awe Formation unconformably with contact in some sections described as gradational (Nwajide, 2013; Offodile, 1989). The commencement of widespread marine transgression into the Trough in the Late Cenomanian is represented by Turonian Eze-Aku Formation comprised of massive flaggy calcareous to non-calcareous shale, sandy or shaley limestone and calcareous sandstones. Accordingly, the Eze-Aku Formation overlies the Keana Formation (Nwajide, 2013; Offodile & Reyment, 1977). The Eze-Aku Formation is in turn overlain by Late Turonian—Coniacian fissile shale dominated sediments of the Awgu Formation that terminated marine sedimentation in this segment of the Trough. The continental sediments of the post-folding Campano-Maastrichtian Lafia Formation lies unconformably on the shale dominated-coal bearing Awgu Formation (Nwajide, 2013; Obaje, 2009). The Lafia Formation is essentially composed of sandstones of varied facies with intercalations of clays. The Lafia Formation is the youngest and is lithologically characterized by widespread ferruginization (Offodile, 1989; Zaborski, 1998). Also, there was widespread volcanic activities within the Trough during the Tertiary era (Nwajide, 2013; Obaje, 2009; Offodile, 1989; Zaborski, 1998). The permeable water yielding sandstone beds of the various formations constitute important aquiferous zones for groundwater withdrawal within the middle Benue Trough (Obrike et al., 2019, Nwajide, 2013, Obaje, 2009, Offodile, 2002, Zaboski, 1998, Obaje, 1994, Offodile, 1976). The occurrence of groundwater within this segment of the Trough is somewhat erratic with potential aquifers either limited in extent, contaminated with brine, with the presence of intercalations of clay and shale or are largely indurated (Nwajide, 2013; Obaje, 2009; Obrike et al., 2022; Offodile, 2002).

Location, geology and physiography of study area

The study area lies between Latitude 8° 26′ 20″ to 8° 35′ 00″ and Longitude 8° 26′ 00″ to 8° 35′ 30″ as shown in Fig. 1. The study area is essentially underlain by the Lafia Formation which is the youngest of the formations in the Middle Benue Trough. The Formation was deposited under fluvio-deltaic (continental) conditions during the Maastrichtian times and lies unconformably on the Late Turonian—Early Santonian coal-bearing Awgu Formation (Nwajide, 2013; Offodile, 1976, 1989). The Lafia Formation is comprised mainly of sandstones of varied facies (ferruginized sandstones, loose sands of the various sand fractions), flaggy mudstones, clays and claystones. The Lafia Formation is the main formation that outcrops in and around the Lafia municipal area. The geological map of the study area is presented in Fig. 1. The sandstone facies are essentially fine to coarse grained, feldspathic, friable, highly porous and permeable, and serves as the primary aquifer in the study area. The poorly consolidated nature of the sandstones renders the Lafia sandstones most prolific amongst the aquifers in the middle segment of the Trough. Average borehole yields of 4.2 L/sec have been reported for wells drilled in the Lafia Formation (Obrike et al., 2022; Offodile, 2002). Offodile, (2002) puts the average thickness of the sandstone aquifer as 150 m and the aquifer is generally recharged directly from rainfall. At shallower depth, the aquifer layers are usually unconfined in nature while artesian conditions exist at depth, as aquifer layers in some locations are often confined by clayey intercalations (Obrike et al., 2019; Offodile, 2002).

The area is largely undulating lowland, drained by River Amba and its seasonal tributaries. Vegetation-wise, the study area is situated within the tropical guinea savannah admixture characterized by isolated trees, shrubs and grasses. The area

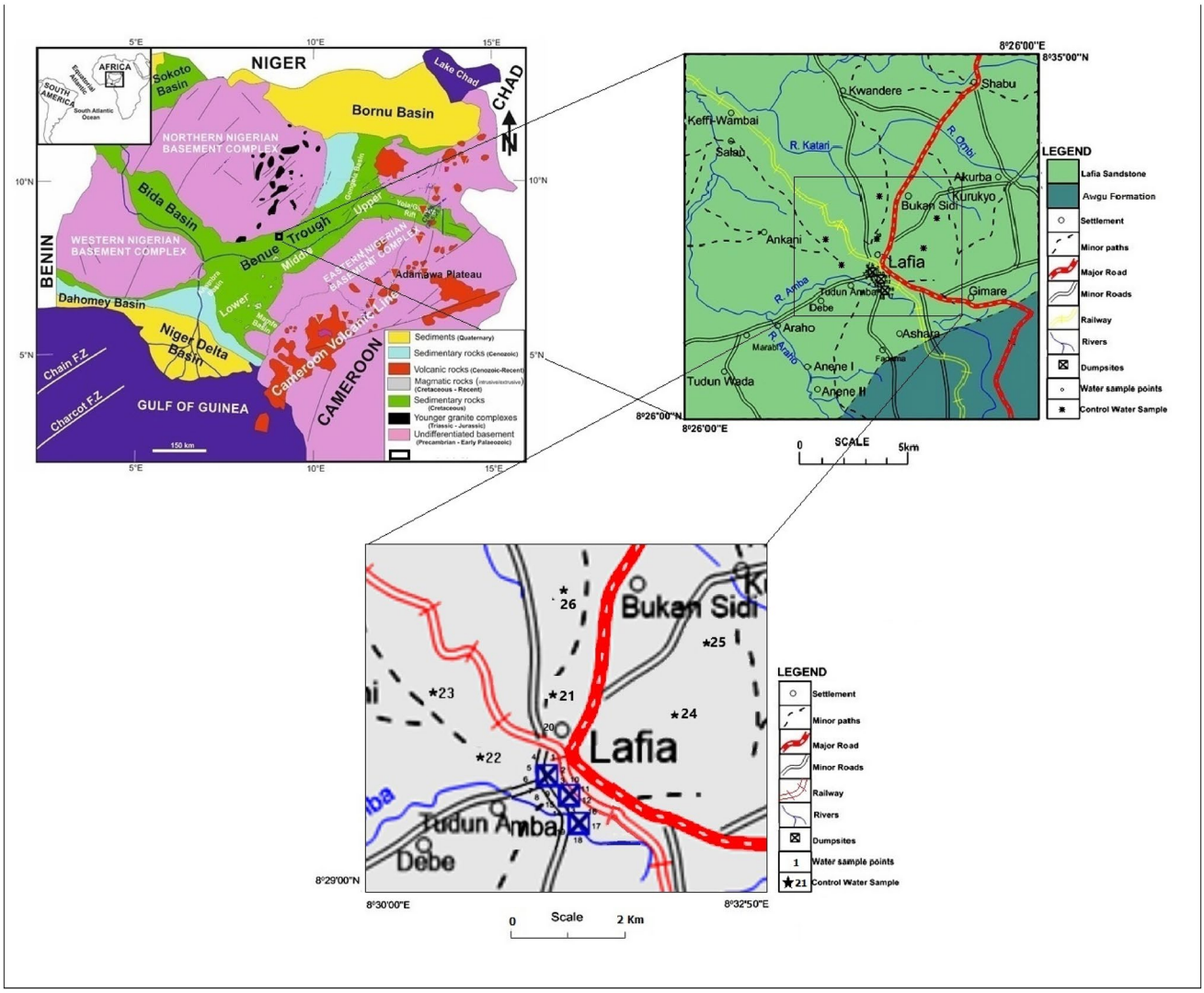

Fig. 1 Location and geological map of the study area

experiences two main climatic conditions annually, namely; the dry and the wet seasons. The dry season begins late October and ends in April, while the wet (rainy) season commences in April, peaks in July and followed by a gradual decline towards October and by November, there is usually little or no rainfall. Generally, the Lafia area is characterized by annual mean minimum temperature in the range of 21.8–22.2 ° C and the annual mean maximum temperature of about 26.5–9.8 °C, with the highest temperatures recorded associated with the months of March and April. The relative humidity values ranges from 88% during the rainy season to about 30% during the dry season.

Sampling and analytical methods

A total of twenty (20) groundwater samples were collected from boreholes, unlined and lined hand-dug wells during dry season at twenty different locations around three non-sanitary dumpsites. The distance of the sampled wells to the nearest dumpsites, type and depth of the wells, alongside the static water levels at the sampled wells were noted. In addition, six (6) control samples were taken from boreholes at about 1 km, 1.5 km, 2 km, 2.5 km, 3 km and 4 km away from any source of leachate contamination (Fig. 1). The groundwater samples were collected in sterilized polypropylene sample containers. Each sample container was thoroughly rinsed out thrice with the water that is to be sampled before the bottle was filled (Anudu et al., 2011; WHO, 2017). In-situ field measurements for temperature, pH, electrical conductivity (EC) and total dissolved solids (TDS) were recorded on site during sampling. EC, TDS and temperature values were determined using TLC Solinsi Deep Metre, Hanna instrument pH 210 was used to determine the pH values in the groundwater samples. Samples collected were afterwards kept under cold conditions in an ice chest and transported same day to the Soil Science Laboratory, Department of Soil Science, Ahmadu Bello University, Zaria, Nigeria at temperature of < 4 °C for laboratory analysis. Preservation of water samples and chemical analyses were carried out using standard procedures as recommended by APHA (2017). The cations, anions and heavy metals concentrations (Ca^{2+}, Mg^{2+}, K^{+}, Na^{+}, Cl^{-}, Cu, Cd, Fe, Mn, Ti, Zn and Pb) were determined using Atomic Absorption Spectrometry method. While concentrations of CO_3^{2-}, NO_3^{2-}, SO_4^{-2}, HCO_3^{-2}, PO_4^{-2} were determined using digital titration methods.

Results and discussion

Physico-chemical characteristics

The results of physical parameters analysed for the various groundwater samples are presented in Table 1. The temperature of the groundwater samples is seen to be in the range of between 28.4 °C and 30.4 °C with a mean value of 29.3 °C. The pH values of analysed groundwater samples ranged between 5.13 and 7.30 (Table 1), with wells in closest proximity to the dumpsites seen to be relatively slightly more acidic in nature. The groundwater samples have an average EC value of 2973 µS/cm and with EC values in the ranges of 89–7754 µS/cm. Largely, the EC values for the sampled lined and unlined wells are higher than the WHO (2017) recommended value of 1000 µS/cm. Also, the EC values appear to decrease with increasing well depth. Nevertheless, wells of close proximity to the dumpsites in comparison with the others exhibited relatively slightly higher EC values at shallower depths. Generally, the TDS values are in the range of 59.63–5195 mg/L with an average value of 1992 mg/L. Most of the wells were characterized by TDS values higher than the WHO (2017) recommended upper limit of 1000 mg/l. The shallow unlined wells exhibited the highest TDS values. Following Todd (1980), with regards to TDS, groundwater quality can be classified as fresh (TDS < 1000 mg/l), brackish (TDS ≥ 1000 ≤ 10,000 mg/l), saline (TDS ≥ 10,000 ≤ 1, 000,000 mg/l); and brine (TDS ≥ 1,000,000 mg/l). Generally, the groundwater samples for wells around the dumpsites are characterized by relatively higher TDS values, with 58% of the total wells categorized as brackish water type and the remaining 42% classify as fresh water type. However, lower TDS values (all within the WHO recommended limits) were recorded for the control wells (48.1 ≤ TDS ≤ 75.6). Dissolved elements emanating for leachates is believed to have significantly contributed to the relatively higher TDS values associated with wells adjoining the landfills. Computed total hardness values for the analysed groundwater samples (after Todd, 1980) ranged between 117 and 722.9 with a mean of 372.

The result of the chemical analysis of the groundwater samples is presented in Table 1. The cations concentrations show the following ranges: Ca^{2+} (47.1–288 mg/L), Mg^{2+} (0.001–1.224 mg/L), K^{+} (0.29–161 mg/L), Na^{+} (0.82–165 mg/L), Ti^{4+} (0.047–4), Fe (0.09–2.67 mg/L), Pb (0–0.362 mg/L), Cd (0–0.002 mg/L), Zn (0–0534 mg/L), Cu (0–0.15 mg/L) and the mean concentration values of the cations is in the order of $Ca^{2+} > Na^{+} > K^{+} > Mg^{2+} > Ti^{4+} > Fe^{(total)}$. Whereas the mean concentration values of the anions are in the order of $SO_4^{2-} > HCO_3^{-} > Cl^{-} > PO_4^{2-} > CO_3^{-}$. The analysed trace elements show a mean concentration order of Pb > Zn > Cu > Cd.

Hydro-geochemical classification

Generally, groundwater condition in an aquifer is a function of the nature of recharge (amount, duration, intensity of precipitation), depth of weathering, resident time, specific

Table 1 Descriptive statistics of measured physical, chemical and trace element concentrations in groundwater samples from areas adjoining the landfills and the six control wells

Parameters	Min	Max	Mean	Standard deviation	WHO (2017)	NSDWQ
Temperature	28.4	30.4	29.3	1.64	Ambient	Ambient
pH	5.2	7.3	6.09	0.61	6.5–8	6.5–8
EC	89	7754	2973	2227.26	1000	1000
TDS	59.63	5195	1992	1492.70	600–1000	1000
Ca^{2+}	47.1	288	146.52	80.40	200	200
Mg^{2+}	0.02	1.23	0.71	0.45	0.2	0.2
K^{+}	0.29	161	53.17	40.74	10	10
Na^{+}	0.82	236	74.58	57.17	200	200
$CO3^{2-}$	0	1.2	0.19	0.34	250	250
$HCO3^{2-}$	0.6	12.2	2.88	3.13	250	250
Cl^{-}	0.2	5.9	2.08	1.47	250	250
$SO4^{2-}$	0.24	42.32	17.55	13.35	100	100
$NO3^{2-}$	0.011	0.19	0.04	0.05	50	50
$PO4^{2-}$	0.42	1.61	0.81	0.31	5	5
Li	0.47	3.10	2.1515	0.998	0.774	0.6
Fe	0.091	2.670	0.4453	0.697	0.3	0.3
Mn	0.0007	0.6282	0.1826	0.192	0.2	0.2
Zn	0.0002	0.5344	0.1066	0.144	3	3
Cu	0	0.1483	0.0117	0.033	1	1
Cd	0	0.0029	0.0012	0.001	0.003	0.003
Pb	0.0075	0.3627	0.1531	0.110	0.01	0.01

*NSDWQ (2016) Nigerian Standard for drinking water, WHO (2017) World Health Organization standards for drinking water. All values are in mg/L except pH, temperature (°C) and EC (µS/cm)

yield and general slope of formation toward drainage channels (Subba Rao, 2006). However, in specific terms, the concentration of chemical components in natural groundwater depends on intricate processes and conditions, such as the availability and solubility of minerals, geochemical environment (e.g. pH and Eh) and exchange processes (Freeze & Cherry, 1979; Subba Rao, 2006). The hydro-geochemical character (evolution and processes) of the sampled groundwater was evaluated using ionic ratios and scatter plots, the Piper (1944) trilinear plot, the Schoeller (1977) diagram, the Durov plot and the Gibbs diagram.

The hydro-geochemical facies generally reflect the effects of the lithological influence on the chemical processes and overall groundwater flow patterns (Clake, 2015, Subba Rao, 2006). The major cations and anions concentrations were converted into milli-equivalent per litre (meq/L) and expressed as percentage of total cations in meq/L. These were employed in the plotting of the existing water facies types in the study area using the Piper (1944) trilinear diagram. The Piper plot reveals Ca^{+} and Na^{+} as the dominant cations whereas SO_4–Cl and HCO_3 are the dominant anions in all of the waters. Also three water types were identified, namely; Ca–Cl–SO_4 water, Ca–Na–HCO_3^{-} mixed water and Na–Cl–SO_4 water types (Fig. 2a). The dominant water types suggest some elements of mixing of high salinity-water with bicarbonate water (Kumar et al., 2014). The Piper trilinear plot also shows that the alkaline earth metals (Ca and Mg) slightly exceed the alkali metals (Na and K) while the strong acids (Cl and SO_4) are relatively more dominant in contrast with weak acids (HCO_3 and CO_3). The relative dominance of the non-carbonate groundwater facies types over the carbonate varieties in the sampled wells adjoining the landfills, suggest a trend in groundwater quality from "fresh to brackish" with increasing proximity to the landfills. The trend reflects the influences of geogenic and anthropogenic activities on the groundwater system (Clake, 2015; Subba Rao, 2006).

The Schoeller diagram showing the relative concentrations of cations and anions of multiple samples from the various wells expressed in milli-equivalent per litre is presented in Fig. 2b. The Schoeller diagram indicates the predominance of Ca^{2+} and $SO4^{2-}$, with cations and anions concentrations occurring in the order of $Ca^{2+} > Na^{+} > Mg^{2+}$ and $SO_4^{2-} > HCO_3^{-} > Cl^{-}$. The prevalence of alkaline earth and alkali elements is commonly indicative of the dissolution of calcium-bearing minerals and alkali-feldspar minerals in the water system (Igwe & Omeka, 2021; Mgbenu & Egbueri, 2019). The sandstones that constitute the aquifers in the Lafia Formation are continental, immature and commonly rich in alkali and plagioclase feldspars (Nwajide, 2013; Obrike et al., 2019; Offodile, 1976, 1989).

The Durov diagram proffers the dominant hydrochemical processes affecting the groundwater chemistry (Fig. 3,

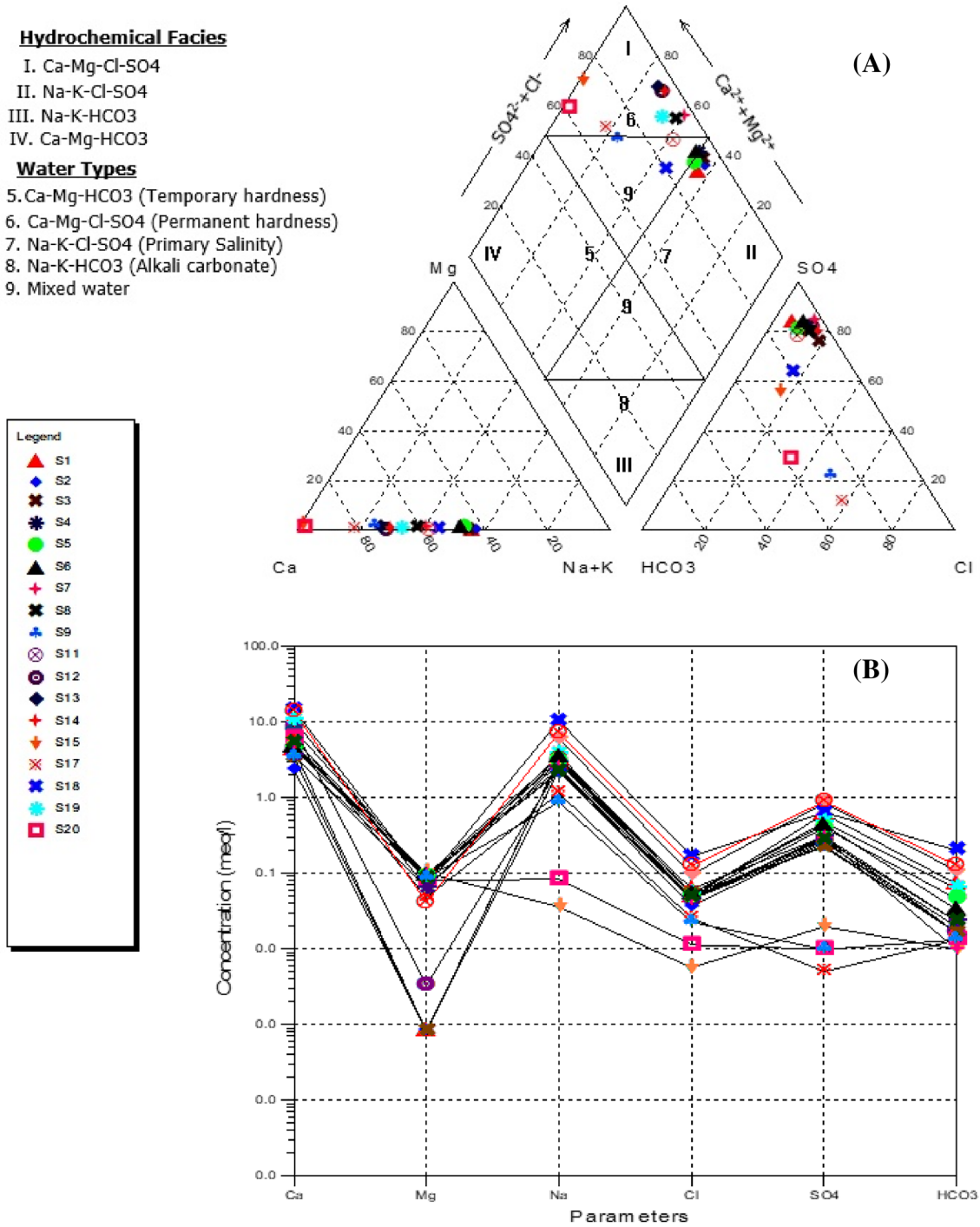

Fig. 2 **a** Piper trilinear diagram showing hydro-geochemical character and hydrochemical facies in the groundwater of study area and **b** Schoeller diagram showing the relative concentrations of cations and anions for various groundwater samples of the study area

Table 3). The Durov diagram indicates that majority of the water samples plot in the fields of simple dissolution and mixing (fields 4 and 5), however, a few other samples indicate the Cl^- dominant anion and Na^+ dominant cation (fields 7 and 8). Elevated values of Na^+ and Cl^- in groundwater can result from a number of sources, but for the study area, contributions from wastewaters and weathering of rocks are adduced to be the primary sources at these locations. The samples within fields 7 and 8 of the Durov diagram suggest the existence of reverse ion exchange processes within the groundwater flow regime where Ca^{2+} and Mg^{2+} in the aquifer matrix have been replaced by Na^+

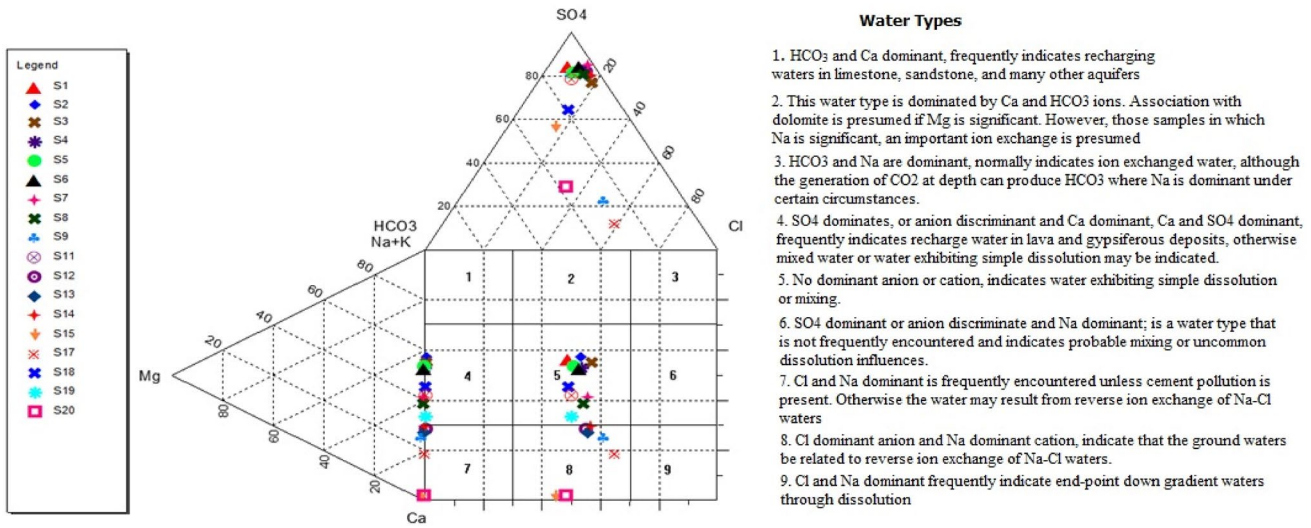

Fig. 3 Durov diagram showing the dominant hydro-geochemical processes affecting the groundwater chemistry in the study area

and K^+ from the water at suitable exchange sites (Zaidi et al., 2015).

The influence of rock-water interaction (lithology and degree of weathering), evaporation and precipitation on the evolution of the hydro-geochemistry of collected groundwater samples are easily discriminated using the Gibbs plot. Gibbs (1970) recommended a plot of total dissolved solids (TDS) against the weight ratio of $Na^+/(Na^+ + Ca^{2+})$ and $Cl^-/ Cl^- + HCO_3^-$. The Gibbs plots of the weight ratios of the cations and anions of the groundwater samples are presented in Fig. 4. The plots suggest chemical weathering of rock forming minerals and to some extent evaporation as pivotal factors driving the evolution of the groundwater geochemistry of the study area. Typically, a normal sequence of groundwater evolution along flow paths with increasing time, is the tendency of groundwater chemistry to change from HCO_3^- type to Cl^- type water with increasing salinity. This process is often accompanied by a change in the dominant cation from Ca^{2+} to Na^+ (Freeze & Cherry, 1979; Clake, 2015; Subba Rao, 2006). The evolution of groundwater water from zones of recharge—precipitation (low TDS and usually a Na–Cl water type) to a Ca–HCO_3 water type upon interaction with sediments and bedrock usually occurs relatively fast. Nonetheless, within the zone of water–rock interaction, the processes of chemical weathering and/or anthropogenic activities overtime increases TDS (salinity) and samples tend to move from rock dominance to zone of evaporation (Clake, 2015; Subba Rao, 2006). This is trend is visibly evident in Fig. 4.

The scatter plots of the concentrations of the earth alkaline metals $(Ca^{2+} + Mg^{2+})$ against bicarbonate (HCO_3^-) and against bicarbonate plus sulphate $(HCO_3^- + SO_4^{2-})$ provides insight into the prevalent ionic exchange processes in the sampled groundwater flow regime (Fig. 5).

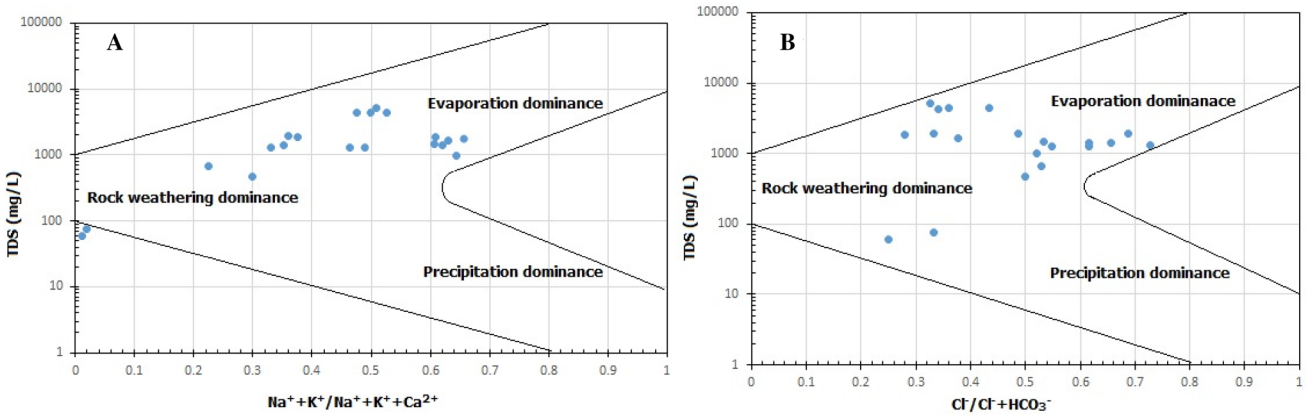

Fig. 4 Gibbs plots showing the evolution of the subsurface water chemistry for dominant cations and anions in the study area

The plot of the earth alkaline metals against bicarbonate ($Ca^{2+} + Mg^{2+}$ vs HCO_3^-) reveals all of the data plotted above the (1:1) equiline, signifying excess earth alkaline metals ions over bicarbonate. This suggests extra sources of Ca^{2+} to Mg^{2+} ions balanced by SO_4^{2-} and Cl^- most likely provided by silicate weathering (Zhang et al., 1995: Subba Rao, 2006; Mgbenu & Egbueri, 2019, Igwe & Omeka, 2021). The plot of $Ca^{2+} + Mg^{2+}$ against $HCO_3^- + SO_4^{2-}$ reveals the prevalence of reverse ion exchange processes as groundwater samples are seen to plot left of the 1:1 equiline (Clake, 2015; Subba Rao, 2006; Barzegar et al., 2017; Barzegar et al., 2018). While, if under ion exchange process dominance, the samples generally would have plotted right of the 1:1 equiline due to the excess of $HCO_3^- + SO_4^{2-}$ over $Ca^{2+} + Mg^{2+}$ (Zhang et al., 1995; Clake, 2015; Subba Rao, 2006; Barzegar et al., 2018). The plots of Na/Cl verse EC and $Ca^{2+} + Mg^{2+}$ vs HCO_3^- suggest silicate weathering as the major control for the release of Ca^{2+}, Mg^{2+}, Na^+ and K^+ into the water (Fig. 5c&d). These plots affirm earlier assertions from the Durov and Gibbs diagrams. All water samples show the ratio Ca^{2+}: $SO_4^{2-} + HCO_3^-$ at the boundary of unity (0.98–0.99), suggesting the flow of water through the normal hydrological cycle and influences of anthropogenic activities (Subba Rao, 2006). Largely, the scatter plots reveal a groundwater chemistry that is chiefly controlled by geogenic processes (weathering of silicates and the cation exchange process) with evidence of subsequent modification by anthropogenic sources (Clake, 2015; Subba Rao, 2006; Barzegar et al., 2017; Igwe & Omeka, 2021).

In addition, the computation of chloro-alkaline indices (CA) allowed for the assessment of changes in chemical composition of groundwater along its flow path. Two chloro-alkaline indices (CA1, CA2) for the interpretation of ion exchange between groundwater and host environment had been developed by Schoeller (1965, 1977). The indices computation is given as:

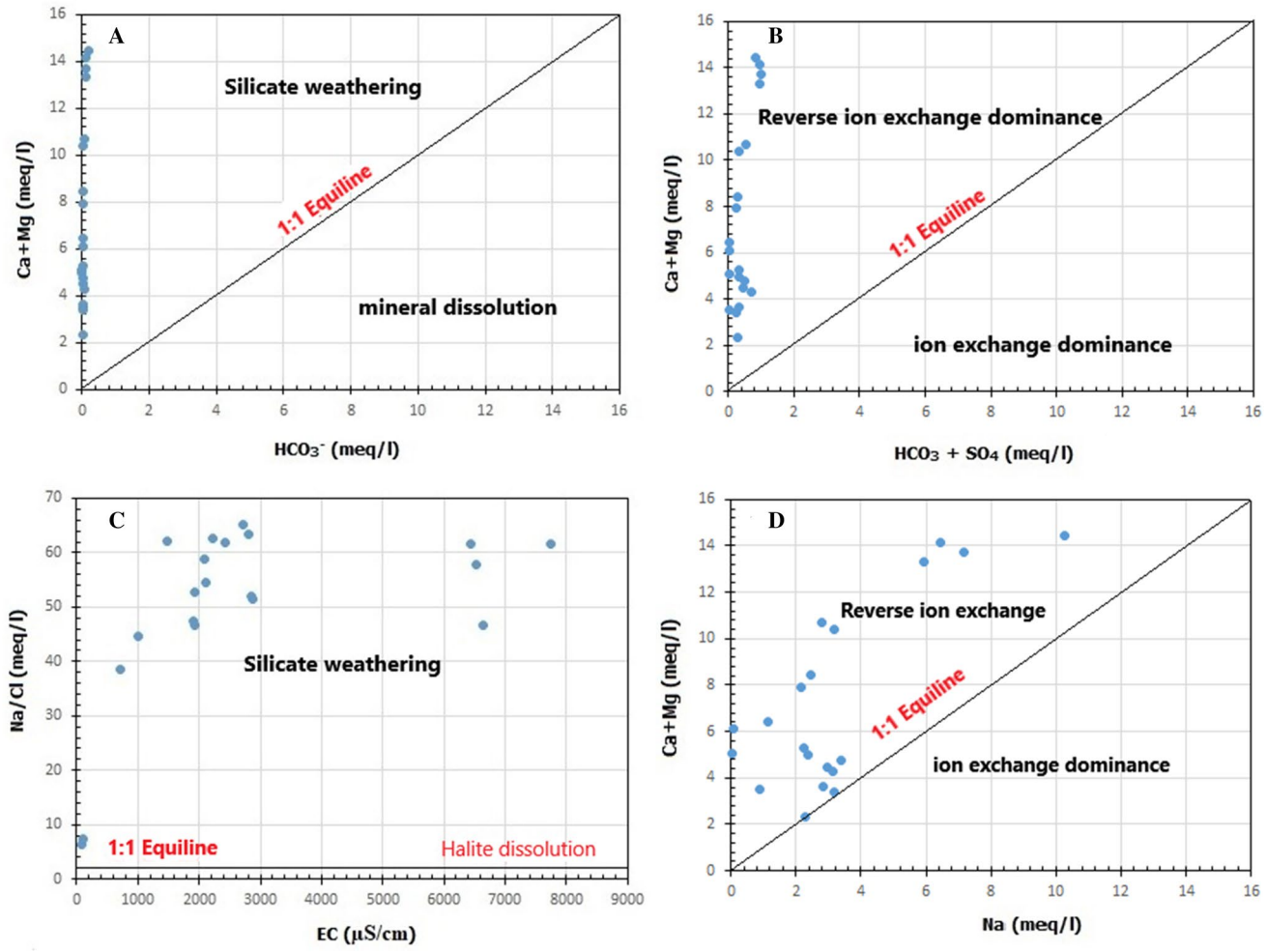

Fig. 5 Scatter plot for ionic ratio of **a** alkali earth (Ca + Mg) against bicarbonate (HCO3), **b** alkali earth (Ca + Mg) against bicarbonate + sulphate (HCO3 + SO4), **c** Na/Cl against EC and **d** alkali earth (Ca + Mg) against sodium (Na)

$$CA1 = \frac{\left(Cl^- - \left(Na^+ + K^+\right)\right)}{Cl^-}, \quad (1)$$

$$CA2 = \frac{\left(Cl^- - \left(Na^+ + K^+\right)\right)}{\left(SO_4^{2-} + HCO_3^-\right)}. \quad (2)$$

Positive CA indices are indicative of the prevalence of reverse ion exchange process signifying the exchange of Na^+ and K^+ from the water with Ca^{2+} and Mg^{2+} of the rocks. While negative values are indicative of chloro-alkaline disequilibrium or cation exchange reactions characterized by an exchange of Ca^{2+} and Mg^{2+} in the water and Na^+ and K^+ from clay minerals in the rocks. All of the groundwater samples exhibited negative CA1 and CA2 values, confirming rock-water interactions as primary source of dissolved ions in the groundwater (Kumar et al., 2014; Subba Rao, 2006; Obrike et al., 2019).

Heavy metal concentration

A total of seven trace metals (Li, Zn, Pb, Cu, Cd, Fe and Mn) were assessed in the collected groundwater samples and the trace metal concentration of the sampled wells is presented in Table 1. The occurrence and mobility of trace metals in groundwater environments is largely influenced by adsorption process related with rock–water interactions and prevalent anthropogenic activities (Mushtaq, 2014). The concentrations in mg/L of Fe (0.1025–2.6708), Mn (0.0007–0.6282), Zn (0–0.5344), Cu (0–0.1483), Cd (0–0.0029), Pb (0.0075–0.3075) and Li (0.47–3.1) show a mean concentration order of Li > Fe > Mn > Pb > Zn > Cu > Cd. Lithium is an alkali metal that naturally occurs in some groundwater as a result of dissolution of lithium bearing minerals and/or interaction with saline or geothermal water (Lindsey et al., 2021). Lindsey et al. (2021) identified that extensive evaporation, mineral dissolution, cation exchange and mixing with geothermal waters or brines may account for lithium enrichment in groundwater. However, very little evidence supports natural sources for lithium enrichment in the study area, as no-known documented evidence of the existence of lithium rich minerals exist in the area. Consequently, the high concentration of lithium in most of the wells around the landfills (above the maximum permissible limits for drinking water) can be traced to anthropogenic sources. Disposed battery cells, television parts, diverse electronics and other industrial materials constitute considerable content of the landfills—some of which had been in place for over 30 years.

The ferruginized nature of sandstones within the Lafia Formation is a characteristic feature (Nwajide, 2013; Obaje, 2009; Obrike et al., 2019; Offodile, 1976). Dissolved Fe from the sandstones, as rain water percolates downwards during the aquifer recharge process, is considered to be the primary source of iron enrichment in the groundwater. Other sources may include Fe-rich leachate from the landfills, which also may have significantly contributed to the elevated levels of the Fe concentrations. Consequently, considerable number of the wells in the study area exhibit higher than normal iron concentrations than that prescribed for drinking water purposes (WHO, 2017). In general, the chemical behavior of Fe and its solubility in water is largely dependent on the oxidation intensity in the groundwater system in which it occurs. Ordinarily, iron encrustation occurs when ferrous iron which is soluble in water undergoes oxidation and are precipitated as ferric iron commonly held in suspension (Clake, 2015; Subba Rao, 2006).

Sixty percent of the sampled groundwater have elevated Mn concentrations higher than normal permissible levels for drinking water (0.05 mg/L). Common sources of Mn in groundwater include weathering of Mn bearing minerals in rocks, industrial effluent, sewage and landfill leachate (Kumar et al., 2014). Mn is known to exhibit similar geochemical character in groundwater systems as Fe. The concentration of both elements in groundwater is largely dependent on the existing redox conditions, residence time, well depth and TDS (Luzati et al., 2016). With increased resident time, groundwater gradually changes from oxic to reducing conditions and the reductive dissolution of Fe^{3+} and Mn^{4+} oxides increases the concentrations of Fe and Mn in groundwater (Champ et al., 1979; Luzati et al., 2016). In sedimentary environments—like the study area, Mn has been reported to be relatively more mobile in contrast with Fe, as Fe is more reactive to changes in redox conditions and thus, tends to precipitate faster (Simmonds & Ghasemi, 2007). The sources of Mn in the study area appears to be both geogenic and anthropogenic in nature.

Significant concentrations of Pb, Zn and Cu in groundwater commonly suggest the existence or interaction with relics of sulfide ores along its flow route or related mining activities (PbS–Galana, (Zn, Fe)S–Sphalerite and $CuFeS_2$–Chalcopyrite, FeS_2–Pyrite). Pb concentrations (0.007–0.3627 mg/L) in groundwater of the study area increases with proximity to the landfill. Hence elevated Pb levels in groundwater is strongly suggestive of origins from anthropogenic source such as disposed lead-batteries, paint containers, pencils, toys, etc. In addition, Pb concentrations in all the samples except at a location exceeded the maximum WHO drinking water permissible limits for Pb (0.01 ppm). The concentrations of Zn (0–0.5344 mg/L), Cu (0 and 0.1483 mg/L) and Cd (0–0.0029 mg/L) were all within the permissible limits for drinking water.

Heavy metal pollution assessment

Indicator indices for heavy metals pollution assessment was carried out using the modified heavy metal index (Chaturvedi et al., 2018). The approach is robust, adaptable and allows for evaluation of surface and groundwater suitability for domestic uses based on established baseline values (maximum desirable limits) for heavy metals in each sample location. The modified heavy metal index (m-HMI) allows for the assigning of weights (objectively or subjectively) to the various water quality parameters (variables). In this study, weights were assigned subjectively based on the significance of each trace element (metals) in the overall water quality evaluation and its impact on the human health system (Egbueri et al., 2020; Igwe & Omeka, 2021; Kumar et al., 2015). A weight rating of 1–5 for the various water quality parameters was adopted. Relative weights of the individual parameters and m-HMI values were determined using the following the equations:

$$w_r = w_{i/} \sum_{i=1}^{n} w_i, \tag{3}$$

$$\text{mHMI} = \sum_{i=1}^{n} \left[w_r \times M_i / S_i \right] \times 100, \tag{4}$$

where w_r is relative weight; n is the overall total of analyzed parameters; w_i unit weight factor for the *i*th heavy metal; M_i is the measured concentration value of each parameter in the groundwater samples; S_i is the maximum permissible limits of WHO (2017) for the *i*th parameters.

A summary of the computed m-HMI results is presented in Table 2. The m-HMI values for the various sampled wells range from 61 to 736 with a mean value of 350. Relatively higher m-HMI values are seen to be associated with wells of close proximity to the landfills. However, based on the m-HMI criteria for the evaluation of surface and groundwater suitability for domestic use (Dash et al., 2019; Egbueri et al., 2020; Igwe & Omeka, 2021), 65% of the analyzed groundwater samples is categorized as unsuitable for drinking purposes (m-HMI > 300), while 15% of the samples fall under the good (m-HMI = 50–100) and poor (m-HMI = 100–200) categories each. Typically, the deeper boreholes are characterized by lower m-HMI values in contrast with the shallower hand-dug and lined wells. Higher m-HMI values were seen to be associated with wells of close proximity to the oldest and largest of the three landfills under consideration and also to a lesser extent, along regional groundwater flow direction- south-westward of study area (Nwajide, 2013; Offodile, 2002).

Water quality assessment

The water quality index (WQI) evaluates the overall suitability of surface and groundwater for drinking purposes based on several key parameters of groundwater chemistry. This index provides a single numeric value that expresses the composite influence of measured parameters on the overall water quality for a sampled location. In this technique weights are assigned to key physico-chemical parameters according to the parameters' relative importance in the overall quality of water for drinking water purposes. Assigned weights range from 1 to 5, with 5 indicating maximum influence and 1 representing relative minimum influence. In this study, a maximum weight of 5 was assigned to EC, TDS and Cd; 4 for pH, SO_4 and Pb; 3 for HCO_3, Cl, Zn and Cu; 2 for Ca, Na, K and weight 1 for Mg (Dash et al., 2019; Egbueri et al., 2020; Igwe & Omeka, 2021; Kumar et al., 2015). The WQI computation comprises four stages; computation of relative weights, quality rating scale, sub-index value and the WQI value for the parameter. Relative weights for the various parameters were computed using the following relationship:

Table 2 Summary of the computed modified heavy metal index (m-HMI) and water quality index (WQI) results for the groundwater samples

Index parameter	Range	Class	%Category	Representative samples
m-MHI	< 50	Excellent	Nil	Nil
	50–100	Good	15	1, 17, 20
	100–200	Poor	5	5, 18, 19
	200–300	Very poor	15	3,
	> 300	Unsuitable	65	2, 4, 6, 7, 8, 9, 10, 11, 12, 13, 14, 15, 16,
WQI	< 50	Excellent	5	20
	50–100	Good	5	17
	100–200	Poor	25	1, 2, 3, 5, 19
	200–300	Very poor	30	6, 7, 8, 9, 13, 15
	> 300	Unsuitable	35	4, 10, 11, 12, 14, 16, 18

$$W_i = w_{i/} \sum_{i=1}^{n} w_i, \tag{5}$$

where W_i is the relative weight; w_i is the weight of each parameter and n is the number of parameters.

The quality rating scale (Qi) for each parameter was computed by dividing measured concentration by its respective standards (WHO, 2017) and multiplied the results by 100.

$$Q_i = \left(C_i/S_i\right) \times 100, \tag{6}$$

where Qi is the quality rating; Ci is the measured concentration of each chemical parameter in each sample; Si is the World Health Organization standard for each chemical parameter according to the guidelines (WHO, 2017).

The sub-index value (SI) was determined for each parameter and the computation of WQI is the summation of SI values for each measured parameter in the groundwater sample. The computations are achieved using the following relations:

$$\mathrm{SI}_i = W_i \times Q_i, \tag{7}$$

$$\mathrm{WQI} = \sum_{i=1}^{n} \mathrm{SI}_i, \tag{8}$$

where SIi is the sub-index of ith parameter, Qi is the rating based on concentration of ith parameter and n is the number of parameters.

The results of the computed WQI values for the various sampled locations is presented in Table 2. In addition to the 20 sampled locations around the landfills, results of the six control sample points are presented alongside for an overview of the water quality of the general adjoining areas (Table 3). The results show that out of the 20 groundwater samples analyzed for WQI, 35% of the sampled locations (essentially composed of hand dug and concrete lined wells in close proximity to the landfills) have water categorized as unsuitable (WQI > 300). These wells are characterized by relatively higher TDS, EC and m-HMI values. 30% of the sampled groundwater locations were characterized by water classified as very poor (WQI = 200–300). These locations comprised of deeper hand-dug wells and motorised borehole schemes are relatively further (200–500 m) from any of the considered landfills. In addition, 25% of the water samples fell under the poor water category (WQI = 100–200). While the good and excellent water categories both constitute 5% each of the total groundwater analysed. Water quality is seen to improve with increased distance from the landfills as demonstrated by the relative improvement (relatively lower m-HMI values) in the computed WQI values for the six control sample locations.

Table 3 Water quality index (WQI) classification for individual well sample and the control samples

Sample ID	Distance from landfill (m)	WQI value	Classification type
W1	25	128.69	Poor
W2	60	187.21	Poor
W3	110	180.91	Poor
W4	120	327.36	Unsuitable
W5	65	163.32	Poor
W6	50	238.02	Very poor
W7	22	292.70	Very poor
W8	20	236.00	Very poor
W9	25	235.03	Very poor
W10	15	370.22	Unsuitable
W11	22	419.25	Unsuitable
W12	50	379.83	Unsuitable
W13	40	264.65	Very poor
W14	18	404.95	Unsuitable
W15	24	204.67	Very poor
W16	280	310.10	Unsuitable
W17	300	74.85	Good
W18	260	332.61	Unsuitable
W19	280	151.99	Poor
W20	600	43.11	Excellent
C21	1500	22.33	Excellent
C22	1000	64.54	Good
C23	2000	24.62	Excellent
C24	2500	54.23	Good
C25	3000	43.57	Excellent
C26	4000	46.15	Excellent

C21 control well, *W1* sampled well

Geo-statistical correlation

Geo-statistical analyses were performed on the measured physico-chemical parameters in an attempt to establish the similarities and differences between the groundwater samples. Pearson's correlation provided a means of evaluating the strength, as well as linearity that exist between all the measured hydro-geochemical parameters. The Pearson's correlation matrix is presented in Table 4. The correlation matrix shows moderate to high positive linearity between Ca, Na, K, HCO_3, SO_4 and Cl, suggestive of existence of mixed water types as indicated by the Durov diagram. There appears not to be any significant influence of pH on the individual concentrations of the trace elements with the exception of Fe (0.41) that portrays a very weak correlation. However, moderate correlation is seen to exist between the trace elements (Li, Mn, Cu), EC and TDS.

Table 4 Correlation coefficient matrix of major cations, anions and trace elements of the study area

	pH	EC	TDS	$CO3^{2-}$	$HCO3^{2-}$	$NO3^{2-}$	Cl^{-}	$SO4^{2-}$	$PO4^{2-}$	Ca^{2+}	Mg^{2+}	K^{+}	Na^{+}	Li	Fe	Mn	Zn	Cu	Cd	Pb
pH	1																			
EC	−0.18856	1																		
TDS	−0.18857	1	1																	
$CO3^{2-}$	0.127222	0.445885	0.445852	1																
$HCO3^{2-}$	−0.12022	0.921235	0.921255	0.465749	1															
$NO3^{2-}$	0.212846	0.464859	0.464829	0.212925	0.360619	1														
Cl^{-}	−0.23111	0.976201	0.976211	0.367678	0.912366	0.415192	1													
$SO4^{2-}$	−0.09229	0.915444	0.915421	0.688822	0.81051	0.534046	0.844992	1												
$PO4^{2-}$	0.066924	0.171614	0.171608	0.328561	0.252832	0.101475	0.094253	0.305066	1											
Ca^{2+}	0.014246	0.836813	0.836811	0.314765	0.769049	0.326781	0.814618	0.709364	0.007526	1										
Mg^{2+}	−0.39579	−0.17398	−0.17396	−0.32045	−0.13232	−0.10324	−0.09686	−0.26907	−0.07267	−0.02704	1									
K^{+}	−0.10976	0.803306	0.803272	0.68321	0.672457	0.460218	0.677024	0.93355	0.429429	0.582736	−0.34737	1								
Na^{+}	−0.18389	0.971876	0.97189	0.34545	0.933407	0.439105	0.981238	0.843165	0.1653	0.756756	−0.1629	0.696923	1							
Li	0.038559	0.630109	0.6301	0.313163	0.573793	0.168418	0.594665	0.544332	−0.00834	0.925872	0.131591	0.47034	0.504129	1						
Fe	0.401552	−0.17938	−0.17937	−0.14127	−0.14079	−0.1251	−0.17589	−0.20423	−0.25842	0.009479	−0.05879	−0.24674	−0.18006	0.07953	1					
Mn	−0.14096	0.555257	0.555248	0.352229	0.518762	0.39602	0.615851	0.527633	−0.28263	0.576206	0.131782	0.304525	0.512303	0.547324	−0.12888	1				
Zn	0.002123	−0.39206	−0.39206	−0.25366	−0.35793	−0.3278	−0.36658	−0.40781	−0.28768	−0.07676	0.405043	−0.44117	−0.43582	0.085168	0.588179	−0.1188	1			
Cu	−0.24864	0.524493	0.524559	−0.13244	0.704324	−0.04533	0.608494	0.225037	0.003074	0.421203	0.12868	0.056898	0.659169	0.226264	0.009638	0.187495	−0.14129	1		
Cd	0.28296	0.101005	0.101027	−0.00335	0.162483	−0.246	0.124869	−0.0006	−0.13253	0.221839	−0.44123	−0.06418	0.123174	0.203986	0.516869	0.028791	−0.01285	0.285509	1	
Pb	−0.10501	−0.1781	−0.17812	−0.44695	−0.39659	0.101914	−0.18326	−0.19491	−0.38381	−0.14398	0.120119	−0.18716	−0.17693	−0.20863	0.296957	−0.21909	0.35782	−0.19481	−0.13205	1

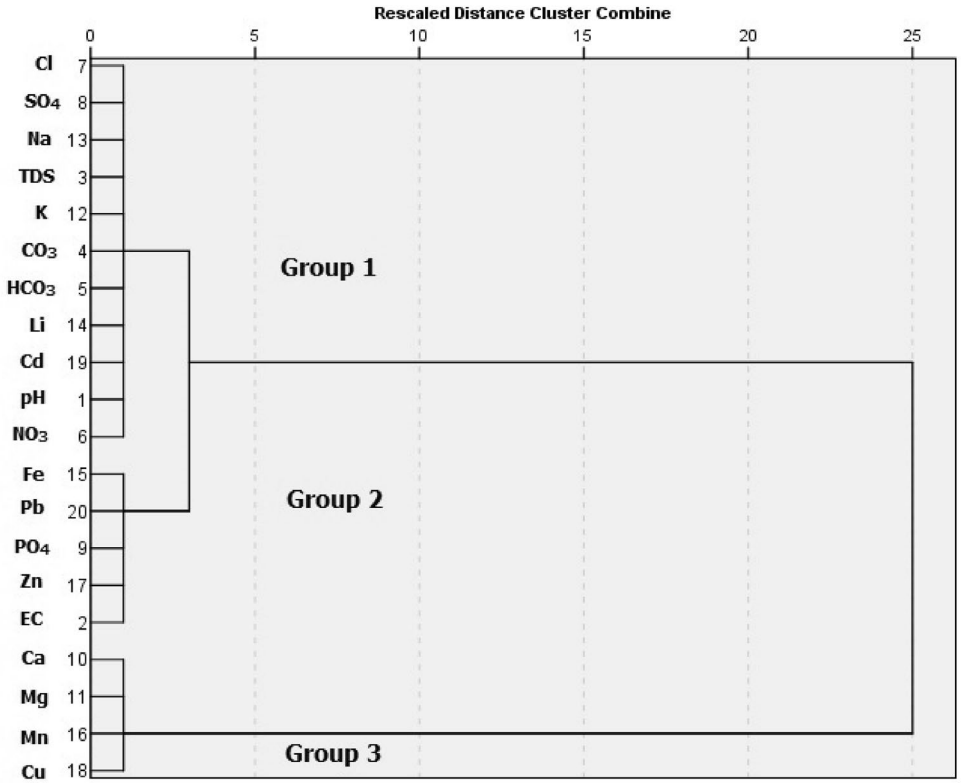

Fig. 6 Dendrogram of groundwater groupings with respect to the measured physico-geochemical parameters in the study area

Cluster analysis employing the hierarchical tree clustering approach was used to group groundwater samples into significant clusters. The unsupervised pattern recognition procedure exposes the inherent structure within a data set by classifying data elements into groups or clusters based on their similarities. The resultant dendrogram was developed using the Ward's minimum-variance method. The dendrogram analysis classified the physico-chemical parameters into three clusters (Fig. 6). A group I cluster comprised of the alkali metals (K, Na, Li), pH, TDS and two sub-groups of anions (Cl, SO_4 and HCO_3, CO_3). A group III cluster comprised of the earth alkali metals (Ca, Mg) closely related to the HCO_3, CO_3 anion sub-group in cluster I. This is responsible for salt combination for the Ca–Cl–SO_4 water, Ca–Na–HCO_3^- mixed water and Na–Cl–SO_4 water types identified in the study area. The group II cluster essentially comprised of trace metals shows strong correlation with EC, pH and possibly suggestive of anthropogenic sources. The proximity of clusters shows good correlation (similarities) between the trace elements (Li, Mn, Cu, Fe, Pb, Zn), EC and TDS, which are the key parameters that influenced the groundwater usability.

Conclusion

Twenty groundwater samples from areas around three non-sanitary landfills were collected, analysed and assessed for drinking purposes. Results of measured physico-chemical parameters show the pH value of the groundwater as slightly acidic to neutral in nature. Following Todd (1980) TDS classification, the groundwater samples were essentially fresh to brackish in nature. The order of abundance of major cations and anions are $Ca^{2+} > Na^{+} > Mg^{2+}$ and $SO_4^{2-} > HCO_3^{-} > Cl^{-}$, while the dominant water types in the study area suggests some elements of mixing of high salinity-water with bicarbonate water. The Durov, Gibbs and scatter plots reveal a groundwater chemistry that is largely controlled by geogenic processes (weathering of silicates and the cation exchange process) with evidence of subsequent modification by anthropogenic sources. Heavy metal pollution assessment reveals relatively higher m-HMI values for wells of close proximity to the landfills, with 65% of the analysed groundwater samples categorized as unsuitable for drinking purposes (m-HMI > 300). While, 15% of the groundwater samples were categorized as poor (m-HMI = 100–200) and another 15% of the samples classed as good (m-HMI = 50–100). Based on the WQI classification, 35% of the groundwater sampled locations have water categorized as unsuitable for drinking purposes. While the

good and excellent water categories both constitute 5% each of the total groundwater analysed.

Acknowledgements The authors are grateful to the anonymous reviewers for their useful suggestions which have greatly improved the revised manuscript.

Funding No funding was received to assist with the preparation of this manuscript.

Availability of data and materials All data and materials as well as software application that were used during the production of the manuscript are available with the authors.

Declarations

Conflict of interest The authors have no conflicts of interest to declare that are relevant to the content of this article.

Ethical approval The research did not involve human participants and/or animals.

Consent to participate The corresponding author has the consent of all the co-authors with regards to their participation in the submission of the manuscript.

Consent for publication The corresponding author has the consent of all the co-authors to liaise on their behalf the editors of the journal with regards the publication of the submitted manuscript.

References

Anudu, G. K., & Obrike, S. E. (2021). Upper lithospheric structure of the middle Benue Trough, Nigeria, derived from analysis of satellite gravity data. *Journal of Mining and Geology, 57*(2), 407–427.

Anudu, G. K., Obrike, S. E., Onuba, L. N., & Ikpokonte, A. E. (2011). Hydrochemical analysis and evaluation of groundwater quality in Angwan Jeba and its environs, Nasarawa State, north-central Nigeria. *Research Journal of Applied Sciences, 6*(2), 128–135.

Anudu, G. K., Stephenson, R. A., Ofoegbu, C. O., & Obrike, S. E. (2020). Basement morphology of the middle Benue Trough, Nigeria, revealed from analysis of high-resolution aeromagnetic data using grid-based operator methods. *Journal of African Earth Sciences, 162*, 1–26.

APHA. (2017). *American Public Health Association, Standard Methods for the Examination of Water and Waste Water* (23rd ed.). Apha.

Barzegar, R., Moghaddam, A. A., Adamowski, J., & Nazemi, A. M. (2018). Assessing the potential origins and human health risks of trace elements in groundwater: A case study in the Khoy plain Iran. *Environmental Geochemistry and Health., 41*, 981–1002.

Barzegar, R., Moghaddam, A. A., Tziritis, E., Fakhri, M. S., & Soltani, S. (2017). Identification of hydrogeochemical processes and pollution sources of groundwater resources in the Marand plain, northwest of Iran. *Environment and Earth Science, 76*, 297.

Benkhelil, J., Dainelli, P., Ponsard, J. F., Popoff, M., & Saugy, L. (1988). The Benue Trough: wrench-fault related basin on the border of the equatorial Atlantic. In W. Manspeizer (Ed.), *Triassic-Jurassic Rifting: Continental Breakup and the Origin of the Atlantic Ocean and Passive Margin. Part A, Developments in Geotectonics 22* (p. 998). Elsevier Science Publishers B. V.

Benkhelil, J., Guiraud, M., Ponsard, J. F., & Saugy, L. (1989). The Bornu–Benue Trough, the Niger Delta and its offshore: tectono-sedimentary reconstruction during the cretaceous and tertiary from geophysical data and geology. In C. A. Kogbe (Ed.), *Geology of Nigeria (2nd Revised Edition)* (pp. 277–309). Rock View (Nigeria) Ltd.

Bodrud-Doza, M., Islam, A. R. M. T., Ahmed, F., Das, S., Saha, N., & Rahman, M. S. (2016). Characterization of groundwater quality using water evaluation indices, multivariate statistics and geostatistics in central Bangladesh. *Water Sciences, 30*, 19–40.

Burke, K. C., & Dewey, J. F. (1974). Two plates in Africa during the Cretaceous? *Nature, 249*, 313–316.

Burke, K. C., & Whiteman, A. J. (1973). Uplift, rifting and the breakup of Africa. In D. H. Tarling & S. K. Runcorn (Eds.), *Implications on Continental Drift to Earth Sciences* (pp. 735–755). Academic Press.

Champ, D. R., Gulens, J., & Jackson, R. E. (1979). Oxidation-reduction sequence in groundwater flow systems. *Canadian Journal of Earth Sciences., 16*, 12–23.

Chaturvedi, A., Bhattacharjee, S., Kumar, A., Singh, A., & Kumar, V. (2018). A new approach for indexing groundwater heavy metal pollution. *Ecological Indicators, 87*, 323–331.

Clake, I. (2015). *Groundwater geochemistry and isotopes*. CRC Press Taylor & Francis Group.

Dahlin, T. (2001). The development of DC resistivity imaging techniques. *Computers and Geosciences, 27*, 1019–1029.

Dash, S., Borah, S. S., & Kalamdhad, A. (2019). A modified indexing approach for assessment of heavy metal contamination in Deepor Beel India. *Ecological Indicators, 106*, 105444.

Egbueri, J. C., Ukah, B. U., Ubido, O. E., & Unigwe, C. O. (2020). A chemometric approach to source apportionment, ecological and health risk assessment of heavy metals in industrial soils from southwestern Nigeria. *International Journal of Environmental and Analytical Chemistry*. https://doi.org/10.1080/0306319.2020

Essien, B. I., Obrike, S. E., Anudu, G. K., & Iyakwari, S. (2011). Preliminary appraisal of chemical and geotechnical properties of clay deposits in Doma area, Middle Benue Trough Nigeria. *International Journal of Chemical Science., 4*(1), 187–195.

Fairhead, J. D., & Binks, R. M. (1991). Differential opening of the central and south atlantic oceans and the opening of the West African Rift system. *Tectonophysics, 187*, 191–203.

Freeze, R. A., & Cherry, J. A. (1979). *Groundwater*. Prentice Hall.

Gibbs, R. J. (1970). Mechanism controlling world water chemistry. *Sciences, 170*, 795–840.

Guiraud, R., Bosworth, W., Thierry, J., & Delplanque, A. (2005). Phanerozoic geological evolution of northern and central Africa: An overview. *Journal of African Earth Sciences, 43*, 83–143.

Guiraud, R., & Maurin, J.C., (1992). Early cretaceous rifts of western and central african. In: Ziegler, P.A. (ed.), *Geodynamics of Rifting, vol. II. Case History Studies on Rifts: North and South America and Africa*. Tectonophysics. 213, pp 153–168.

Guiraud, R., & Maurin, J. C. (1993). Cretaceous rifting and basin inversion in Central Africa. In U. Thorweihe & H. Schandelmeier (Eds.), *Geoscientific Research in Northeast Africa* (pp. 203–206). A. A Balkema.

Igwe, O., & Omeka, M. E. (2021). Hydrogeochemical and pollution assessment of water resources within a mining area, SE Nigeria, using an integrated approach. *International Journal of Energy and Water Resources.* Available online 26 Dec 2020.

Kumar, S. K., Logeshkumaran, A., Magesh, N. S., Godson, P. S., & Chandrasekar, N. (2014). Hydrogeochemistry and groundwater quality appraisal of part of south Chennai coastal aquifers, Tamil Nadu, India using WQI and fuzzy logic method. *Applied Water Science, 4*, 341–350.

Kumar, S. K., Logeshkumaran, A., Magesh, N. S., Godson, P. S., & Chandrasekar, N. (2015). Hydro-geochemistry and application of

water quality index (WQI) for groundwater quality assessment, Anna Nagar, part of Chennai City, Tamil Nadu India. *Applied Water Science., 5*, 335–343.

Lindsey, B.D., Belitz, K., Cravotta, C.A., Toccalino, P.L., & Dubrovsky, N.M. (2021). Lithium in groundwater use for drinking—water supply in the United States. Science of the Total Environment, 767, available online 26 December 2020.

Lloyd, J. A., & Heathcote, J. A. (1985). *Natural Inorganic Hydrochemistry in Relation to Groundwater: An Introduction* (p. 296). Press, New York.

Luzati, S., Beqiraj, A., Beqiraj, G. E., & Jaupaj, O. (2016). Iron and Manganese in groundwater of Rrogozhina Aquifer, Western Albania. *Journal of Environmental Science and Engineering., 5*, 276–285.

Mgbenu, C. N., & Egbueri, J. C. (2019). The hydrogeochemical signatures, quality indices, and health risk assessment of water resources in Umunya district, southeast Nigeria. *Applied Water Science, 9*(1), 22.

Mushtaq, H. (2014). Toxic trace element contamination in ground water of Bollaram and Patancheru, Andhra Pradesh India. *American Journal of Chemistry., 4*(1), 1–9.

Nwajide, C.S. (2013). Geology of Nigeria's Sedimentary Basins. CSS Press (A division of CSS Bookshops Limited) Lagos Nigeria. p. 565.

Obaje, N. G. (1994). Coal Petrography, Microfossils and Paleoenvironments of Cretaceous Coal Measures in the Middle Benue Trough of Nigeria. *Tuebinger Mikropalaeontologische Mitteilungen., 11*, 1–165.

Obaje, N. G. (2009). *Geology and Mineral Resources of Nigeria*. Springer.

Obrike, S. E., Maina, B. M., & Ofoegbu, C. O. (2019). Mineralogical, geochemical and geotechnical characteristics of the maastrichtian clay member of the Lafia formation in Doma and Shabu areas, middle Benue Trough. *Journal of Mining and Geology., 55*(2), 109–118.

Obrike, S. E., Oleka, A. B., Ojuola, B. S., Anudu, G. K., Kana, M. A., & Iliya, M. M. (2022). Hydrogeophysical assessment of groundwater potential and aquifer vulnerability of the Turonian Makurdi Formation in North Bank area, Makurdi, middle Benue Trough, Nigeria. *Journal of Mining and Geology., 58*(1), 189–201.

Offodile, M. E. (1976). The geology of middle Benue Trough, Nigeria. *Special Volume, Paleontological Institution of University of Uppsala, 4*, 1–66.

Offodile, M. E. (1989). A review of the geology of the Cretaceous of the Benue Trough. In C. A. Kogbe (Ed.), *Geology of Nigeria* (2nd ed., pp. 265–376). Rock view Nigeria Ltd.

Offodile, M. E. (2002). *Groundwater Study and Development in Nigeria*. Mecon Geology and Eng. Services Ltd.

Offodile, M. E., & Reyment, R. A. (1977). Stratigraphy of the Keana-Awe area of the middle Benue region of Nigeria. *Bulletin Geology, 7*, 37–66.

Olade, M. A. (1975). Evolution of Nigeria's Benue Trough (aulacogen): A tectonic model. *Geological Magazine, 112*(6), 575–583.

Piper, A. M. (1944). A graphic procedure in the geochemical interpretation of water-analyses. *Eos Transactions. American Geophysical Union, 25*, 914–928.

Schoeller, H. (1965). Qualitative evaluation of groundwater resources. *Methods and techniques of groundwater investigations and development* (pp. 54–83). UNESCO.

Schoeller, H., et al. (1977). Geochemistry of groundwater. In R. H. Brown (Ed.), *Groundwater studies—an international guide for research and practice* (pp. 1–18). UNESCO.

Simmonds, V., & Ghasemi, F. (2007). Investigation of manganese mineralization in Idahlu and Jokandy, southwest of Hashtrood NW Iran. *BHM Berg-Und Hüttenmännische Monatshefte, 152*(8), 263–267.

Subba-Rao, N. (2006). *Hydrogeology—Problems with Solutions*. PHI Learning Private Limited.

Todd, D. K. (1980). *Groundwater Hydrology*. Wiley.

WHO. (2017). *WHO Guidelines for Drinking-water Quality* (4th ed.). World Health Organization.

Wright, J. B. (1976). Origins of the Benue Trough—a critical review. In C. A. Kogbe (Ed.), *Geology of Nigeria* (pp. 313–318). Elizabethan Publication Co.

Wright, J. B. (1981). Review of origins evolution of the Benue Trough in Nigeria. *Earth Evolution Sciences., 2*, 98–103.

Zaborski, P. M. (1998). A review of the cretaceous system in Nigeria. *African Geoscience Review, 5*(4), 385–483.

Zaidi, F. K., Nazzal, Y., Jafri, M. K., Naeem, M., & Ahmed, I. (2015). Reverse ion exchange as a major process controlling the groundwater chemistry in an arid environment: A case study from northwestern Saudi Arabia. *Environmental Monitoring and Assessment, 187*, 607.

Zhang, J., Huang, W. W., Letolle, R., & Jusserand, C. (1995). Major element chemistry of the Huanghe (Yellow River), China: Weathering processes and chemical fluxes. *Journal of Hydrology, 168*, 173–203.